Available online at www.sciencedirect.com

ScienceDirect

IFAC Papers Online CONFERENCE PAPER ARCHIVE

IFAC PapersOnLine 55-33 (2022) 105–110

Map Meshing Impact on the Efficiency of Nonlinear Set-based Model Predictive Control for Water Quality Assessment

A. Anderson [*,**] **J.G. Martin** [***] **N. Bouraqadi** [*] **L. Etienne** [*] **L. Fabresse** [*] **K. Langueh** [*] **G. Lozenguez** [*] **L. Rajaoarisoa** [*] **J.M. Maestre** [***] **E. Duviella** [*]

[*] *IMT Nord Europe, Institut Mines-Télécom, Centre for Digital Systems, F-59000 Lille, France*

[**] *Instituto de Desarrollo Tecnológico para la Industria Química (INTEC), Consejo Nacional de Investigaciones cientficas y tecnicas (CONICET), Santa Fe, Argentina*

[***] *Departamento de Ingeniería de Sistemas y Automática, Universidad de Sevilla, C/ Camino de los Descubrimientos, s/n., 41092 Sevilla, Spain*

Abstract:
Unmanned Surface Vehicles (USVs) are used to collect data of physicochemical parameters used to determine the degradation of freshwater resources. An optimal strategy based on a Nonlinear set-based Model Predictive Control (NMPC) is designed to improve the control of the USVs. This work offers a theoretical novel formulation of NMPC and explains the interest of set-based NMPC. The influence of meshing the map of the area of interest is then studied and it is finally demonstrated that complex trajectories, i.e. spiral or u-turn or even exploring in small areas can be made easy from the control point of view by using hexagonal set-based instead of square NMPCs.

Keywords: Nonlinear MPC, Unmanned Vehicles, Environmental Missions, Water Quality Assessment

1. INTRODUCTION

Water Quality (WQ) assessment requires *real-time* data analysis. Some of the parameters to be analyzed are *Turbidity*, *Dissolved Oxygen*, *PH*, *Conductivity*, and *Temperature*, among others. Also, these parameters can be measured at different depth levels. To Monitor these parameters it is generally necessary to exploit highly reliable instrumentation deployed in few locations. Unfortunately, this strategy is inadequate to evaluate the WQ of large water bodies like the experiments to determine the degradation of the Heron Lake in Villeneuve d'Ascq (France) published on Anderson et al. (2022b). The experiment required a vast collection of reliable data in real-time over a remote area, which represents one of the main challenges to overcome in environment missions Madeo et al. (2020). The latest technological methods for real-time data acquisition is based on Unmanned Vehicles (UV) which provide the appropriate flexibility to explore sophisticated environments efficiently (*see* Wang et al. (2021); Martin et al. (2021) and the references therein).

Model Predictive Control (MPC) is one of the most successful advanced control techniques in the process industries. Its properties have been widely investigated over the last decades, and currently, MPC is a control technique capable of providing stability, robustness, constraint satisfaction, and tractable computation for linear and for nonlinear systems Mayne et al. (2000). Formulating an MPC demands some formal analysis, i.e. the modelling of the *control dynamic system*, the construction of a proper *objective function*, the characterization of a feasible *stabilizable region* and *constraints* consideration on states and inputs. All this implies a full analysis of the problem to be solved. There are several MPC strategies for exploration missions with application to nonholonomic robots, such as the trajectory tracking and path-following Nascimento et al. (2018) or multitarget tracking Sarunic and Evans (2014). The review Matschek et al. (2019) provides a general discussion on covering set-point, trajectory tracking, path-following and their approaches within the Nonlinear Model Predictive Control (NMPC) framework which enables efficient navigation with UV. However, most of the literature on NMPC for exploration is based on set-point stabilization rather than set-based stabilization. Stabilization of target sets rather than individual points is known to offer some advantages to the controller, such as robustness, flexibility, or larger domain of attraction (Blanchini and Miani, 2015), and it is the best strategy to be used if it is enough to reach at least one state inside a given target region (this is the case of the exploration mission carried out in Anderson et al. (2022b)).

In Anderson et al. (2022a) we formulated a novel set-based NMPC for exploration. The proposal was based on a meshing of the surface to be explored given by a set of squares that covers the whole region. The meshing intended to set up a simple and general offline motion planning. Then, the squares serve as a set of targets to be reached for the controller states, and the value of *Turbidity, Dissolved Oxygen, PH, Conductivity and Temperature* was measured in every square for later analysis. In this work the strategy is assessed for the same exploration mission but for different map meshing of the region of interest. The idea is to prove that using *hexagons* instead of *squares* in the meshing map will impact on the efficiency of the proposed

10.1016/j.ifacol.2022.11.017

controller. Several simulation results aimed at water quality assessment show the properties of the proposed controller and provide some insights into the consideration of different mesh shapes.

1.1 Notation

We denote with $\mathbb{N}$ the sets of integers, $\mathbb{N}_0 := \mathbb{N} \cup \{0\}$ and $I_i := \{0, 1, \dots, i\}$. The ceiling function is defined by $\text{ceil}(x) := \min\{n \in \mathbb{N} : x \leq n\}$. The *close ball with center in* $x \in \mathbb{R}^n$ *and radius* $\varepsilon > 0$ is given by $\mathcal{B}(x, \varepsilon) := \{y \in \mathbb{R}^n : \|x - y\| \leq \varepsilon\}$. The point x is an *interior point of* $\mathcal{U}$ if the there exists $\varepsilon > 0$ such that the open ball $\mathcal{B}(x, \varepsilon) \subseteq \mathcal{U}$. The interior of a set $\mathcal{U}$ is the set of all its interior points and it is denoted by $\text{int}\,\mathcal{U}$.

2. NONLINEAR SYSTEM AND SET-BASED CONTROL

Consider the following discrete-time nonlinear system

$$\begin{cases} x(i+1) & = f(x(i), u(i)), \\ x(0) & = x_0, \end{cases} \tag{1}$$

where $x(i) \in \mathbb{X} \subset \mathbb{R}^n$ is the measured state and $u(i) \in \mathbb{U} \subset \mathbb{R}^m$ the control input at time i. The constraint sets $\mathbb{X}$ and $\mathbb{U}$ are compact and convex with the origin inside and the function $f : \mathbb{X} \times \mathbb{U} \to \mathbb{X}$ is continuous with $f(0, 0) = 0$.

The following definition presents the concept of invariance sets of control.

Definition 1 (Control Invariant Set - CIS)**.** *The set* $\Omega \subset \mathbb{X}$ *is a control invariant set (CIS) for system* (1) *if for all* $x \in \Omega$ *there exists* $u \in \mathbb{U}$ *such that* $f(x, u) \in \Omega$.

A CIS has an associated corresponding input set given by

$$\Psi(\Omega) := \{u \in \mathbb{U} : \exists\, x \in \Omega \text{ such that } f(x, u) \in \Omega\},$$

In addition, a CIS Ω is called a Contractive CIS if for every $x \in \Omega$ there is $u \in \mathbb{U}$ such that $f(x, u) \in \text{int}\,\Omega$.

Before formulating the general set-based MPC let us consider the following definition.

Definition 2 (Generalized Distance Stage Cost Function)**.** *A generalized distance function* $d(x, \Omega)$*, from* x *to the CIS* Ω*, is a function with the following properties: (1)* $d(x, \Omega)$ *is convex* [1] *and continuous for all* $x \in \mathbb{X}$*, (2)* $d(x, \Omega) = 0$ *for all* $x \in \Omega$*, (3)* $d(x, \Omega) > 0$ *for all* $x \in \mathbb{X} \setminus \Omega$.

The cost function can be defined as follow.

$$V_N(x, \Omega; \mathbf{u}) = \sum_{j=0}^{N-1} \alpha d(x_j, \Omega) + \beta d(u_j, \Psi(\Omega)), \tag{2}$$

and thus, the general set-based MPC is given by the following optimization problem solved at each sample time $i \in \mathbb{N}$.

$$\begin{aligned} \min_{\mathbf{u}} \; & V_N(x, \Omega; \mathbf{u}) \\ \text{s.t.} \quad & x_0 = x, \\ & x_{j+1} = f(x_j, u_j), \quad j \in I_{N-1}, \\ & x_j \in \mathbb{X}, \quad u_j \in \mathbb{U}, \quad j \in I_{N-1}, \\ & x_N \in \Omega \end{aligned} \tag{3}$$

where α and β are positive real numbers, N is the prediction horizon, the initial state $x = x_0$, the predicted states $x_{j+1} = f(x_j, u_j)$ and the input sequence $\mathbf{u} = \{u_0, \cdots, u_{N-1}\}$.

[1] Note that function $d(\cdot, \Omega) : \mathbb{X} \to \mathbb{R}_{\geq 0}$ so for its convexity it is necessary to ask that the set Ω is a convex set.

Taking into account the receding horizon policy the control law at time i is given by the first element of the optimal sequence $\mathbf{u}^o$. Consider the next Lemma for asymptotic stability result of the closed-loop system.

Lemma 3. *[Anderson et al. (2022a)] If* $\Omega \subset \mathbb{X}$ *is a CIS for system* (1) *in the cost function* (2)*, then* Ω *is asymptotic stable for the closed-loop system* (1) *controlled by the set-based MPC given by* (3).

3. MULTI-TARGET SET TRACKING

The previous control is extended in this section. Let us suppose that the closed-loop system has to reach every element on the set $\mathbf{\Omega} = \{\Omega_1, \Omega_2, \cdots, \Omega_K\}$ with $\Omega_i \subset \mathbb{X}$ for $i = 1, \cdots, K$, in the specified order.

It is clear that a condition must be established in order to switch target every time the current target is reached. To this end a state-dependent MPC will be used. Consider the following condition that defines if a target set on $\mathbf{\Omega}$ is considered a *reached set* according the position of the current state.

Definition 4 (Reached set)**.** *The first set on* $\mathbf{\Omega}$*, i.e.,* Ω_1 *is considered a* reached set *if* $x(i) \in \Omega_1$ *for some* $i > 0$*. For* $k > 1$*, the target set* $\Omega_k \in \mathbf{\Omega}$ *is considered a* reached set *if* $x(i) \in \Omega_k$ *for some* $i > 0$ *and the previous sets* $\Omega_1, \dots, \Omega_{k-1}$ *are* reached sets.

Now, consider the *current target set*, Ω_x, which depends on the position of the current state $x = x(i)$.

Definition 5 (Current target set)**.** *Consider the sate of the closed-loop system* $x(i) \in \mathbb{X}$ *for* $i = 0, \dots, k$*, where* $x := x(k)$ *is the current state at time* k*. The* current target set*,* Ω_x*, is given by*

$$\Omega_x := \{\Omega_{k+1} : k = \max\{i : \Omega_i \textit{ is a reached set}\}\} \tag{4}$$

In the case that there are not reached sets then $\Omega_x := \Omega_0$.

We are in a position to define a set-based MPC for tracking sets on $\mathbf{\Omega}$.

$$\begin{aligned} \min_{\mathbf{u}} \; & V(x, \Omega_x, \mathbf{u}) \\ \text{s.t.} \quad & x_0 = x, \\ & x_{j+1} = f(x_j, u_j), \quad j \in I_{N-1}, \\ & x_j \in \mathbb{X}, \quad u_j \in \mathbb{U}, \quad j \in I_{N-1}, \\ & x_N \in \Omega_x, \end{aligned} \tag{5}$$

The control law at time i is given by the first element of the optimal sequence $\mathbf{u}^o$ of problem 5. For an asymptotic stability result consider the next Lemma.

Lemma 6. *[Anderson et al. (2022a)] If* $\Omega_j \in \mathbf{\Omega}$ *is a Contractive CIS for all* $j = 1, \dots, K$*, then every* $\Omega_j \in \mathbf{\Omega}$ *is a reached set for the closed-loop system controlled by the MPC given on* (5).

Remark 7. *The proposed multi-target tracking has stability guarantee. However, in order to minimize the cost the velocity of the USV tends to decrease near the current set* Ω_x *and to increase once it reaches it, leading to an unwanted behavior. The next section presents an MPC for tracking that avoids this behaviour and improves the performance of the trajectory.*

4. PROPOSED MPC

The design of the control law presented in this section plans the approach to set Ω_j considering that the next move is to reach the set Ω_{j+1}. For this objective a dual-MPC formulation

is used: the *first mode* aims at reaching the current target set $\Omega_x = \Omega_j$, by means of (5), and *second mode* is activated when the current state x is close enough of Ω_x, this mode increases the importance to reach next target set, i.e. Ω_{j+1}.

To trigger the *second mode* let us define some concepts first.

Definition 8 (Fattening set)**.** *Let $\Omega_x \subset \mathbb{R}^n$ be the current target set of control, and let $\varepsilon > 0$, we denote the* ε-fattening set of Ω_x *by*

$$(\Omega_x)^\varepsilon := \cup\{\mathcal{B}(x,\varepsilon) : x \in \Omega_x\}.$$

Remark 9. *The term 'close enough' of the current target set is a parameter of the control design and can be selected by choosing an appropriate ε.*

The *second mode* is activated when the current state is on $(\Omega_x)^\varepsilon$. At this time is necessary to define a second target set, which follows the current Ω_x. The following properly defines the second target set, Ω_x^+:

Define Ω_x as in Eq. (4), and the set Ω_x^+ as follows:

$$\Omega_x^+ := \begin{cases} \Omega_{j+1}, \text{ being } \Omega_j = \Omega_x, & x \in (\Omega_x)^\varepsilon \\ \Omega_x, & \text{otherwise} \end{cases} \tag{6}$$

Note that, if the current state $x \notin (\Omega_x)^\varepsilon$, then it is considered that $\Omega_x^+ = \Omega_x$. This small detail allow us to formulate the problem in a consistent way.

The strategy of the *second mode* depends on a variable prediction horizon which depends on the current state position. The function $N_x : \mathbb{X} \to \mathbb{I}_N$ defines the prediction horizon of the proposal.

$$N_x := \begin{cases} \text{ceil}(\frac{Nd(x,\Omega_x)}{N}), & x \in (\Omega_x)^\varepsilon \\ ^{\varepsilon}, & \text{otherwise} \end{cases}$$

For the *first mode* ($x \notin (\Omega_x)^\varepsilon$) the prediction horizon is N. For the *second mode* ($x \in (\Omega_x)^\varepsilon$) the prediction horizon decreases with the distance of the current state x to the current target set Ω_x. The $\text{ceil}(\cdot)$ function is considered for N_x to be an integer number.

Remark 10. *Function N_x is a decreasing function with maximum value when x belongs to the complement of $(\Omega_x)^\varepsilon$, given by $N_x = N$; and a minimum value when $x \in \Omega_x$, given by $N_x = 0$.*

Consider the cost function

$$J_N(x;\mathbf{u}) = \sum_{j=0}^{N_x-1} p\ell_{\Omega_x}(x_j,u_j) + \sum_{j=N_x}^{N-1} q\ell_{\Omega_x^+}(x_j,u_j) \tag{7}$$

where $\ell_\Omega(x_j,u_j) := \alpha d(x_j,\Omega) + \beta d(u_j,\Psi(\Omega))$, and $p,q > 0$ are weight values.

The *second mode* computes N_x predictions to minimize the distance of the states to Ω_x and $N - N_x$ predictions to minimize the distance of the states to Ω_x^+.

The proposal is given by the following optimization problem solved at each sample time $i \in N$.

$$\begin{aligned} \min_{\mathbf{u}} \ & J_N(x;\mathbf{u}) \\ \text{s.t.} \ & x_0 = x, \\ & x_{j+1} = f(x_j,u_j), \quad j \in I_{N-1}, \\ & x_j \in \mathbb{X}, \quad u_j \in \mathbb{U}, \quad j \in I_{N-1}, \\ & x_{N_x} \in \Omega_x, \\ & x_N \in \Omega_x^+, \end{aligned} \tag{8}$$

The solution of Problem (8) is the optimal control sequence $\mathbf{u}^0 = \{u_0^0, u_1^0, \cdots, u_{N-1}^0\}$. The proposed control law at time i is given by $\kappa = u_0^0$.

The control algorithm executed at any $i-th$ time instant is the following:

Algorithm 1: Proposed nonlinear MPC algorithm

Data: $N \in \mathbb{N}$, $\mathbb{X} \subset \mathbb{R}^n$, $\mathbb{U} \subset \mathbb{R}^m$, $\mathbf{\Omega} = \{\Omega_j\}_{j=1}^K$
Result: Closed-loop system $x(i+1) = f(x(i),\kappa(i))$
1: Read $x = x(i)$;
2: Compute Ω_x, Ω_x^+ with Eq. (4) and (6);
3: Solve Problem (8);
4: Inject $\kappa(i) = u_0^0$ into the system;
5: $i \leftarrow i+1$;
6: Go back to 1

5. SIMULATIONS RESULTS

The kinematic model for the SPYBOAT® vessel used in the experiments is given by the following equations.

$$\begin{cases} \dot{x} &= u\cos(\psi) - v\sin(\psi), \\ \dot{y} &= u\sin(\psi) + v\cos(\psi), \\ \dot{\psi} &= r, \\ \dot{u} &= \frac{\tau_u}{m_{11}} + \frac{m_{22}}{m_{11}}vr + \frac{X_u}{m_{11}}u, \\ \dot{v} &= -\frac{m_{11}}{m_{22}}ur + \frac{Y_v}{m_{22}}v, \\ \dot{r} &= \frac{\tau_r}{m_{33}} + \frac{m_{22}-m_{11}}{m_{33}}uv + \frac{N_r}{m_{33}}r \end{cases} \tag{9}$$

where (x,y) is the position vector on the surface, ψ is the direction of the vessel, and u,v,r are velocity vectors (surge, sway and yaw respectively). The inputs are given by $\tau_u = F_1 + F_2$ and $\tau_r = b(F_1 - F_2)$, where F_1 and F_2 are the port side and starboard side thrust forces, and b represents $1/2$ of the distance between the thrusters. The parameter X_u, Y_v and N_r are the linear drag coefficient in surge direction from surge, the linear drag coefficient in sway direction from yaw rate and the linear drag moment coefficient from yaw rate, respectively. The mass parameters m_{ii} include added mass contributions that represent hydraulic pressure forces and torque due to the forced harmonic motion of the vessel which are proportional to the acceleration:

$$\begin{aligned} m_{11} =& m + 0.05m, \\ m_{22} =& m + 0.5(\rho\pi D^2 L), \\ m_{33} =& \frac{m(L^2+W^2) + 0.5(0.1mB^2 + \rho\pi D^2 L^3)}{12}. \end{aligned}$$

where m is the actual mass, L is the effective length (hull's length in the water), W is the width, D is the mean submerged depth, B is the distance between propellers and ρ is the water density [2] .

[2] For more detail on the parameters of model (9) see Hervagault (2019).

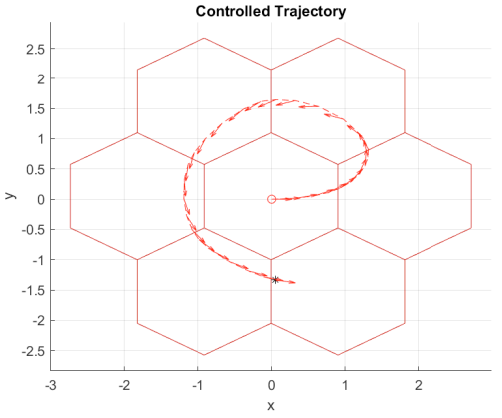

(a) Spiral with hexagon meshing.

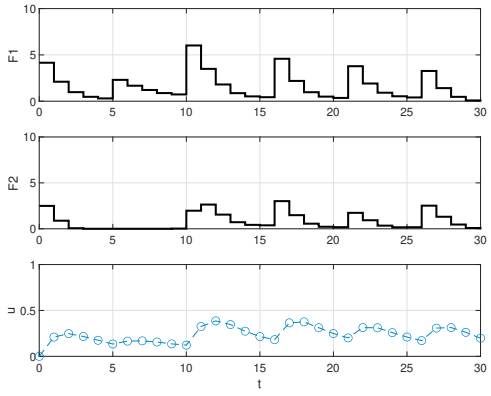

(b) Inputs and velocity u.

Fig. 1. The initial point of the trajectory is given by the ring in the center and the final point by the star. The controlled trajectory follows an spiral sequence of target sets given by hexagons.

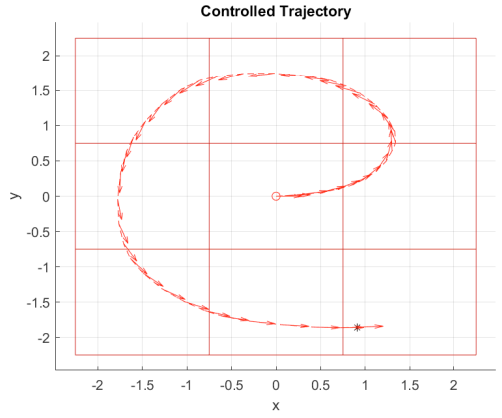

(a) Spiral with square meshing.

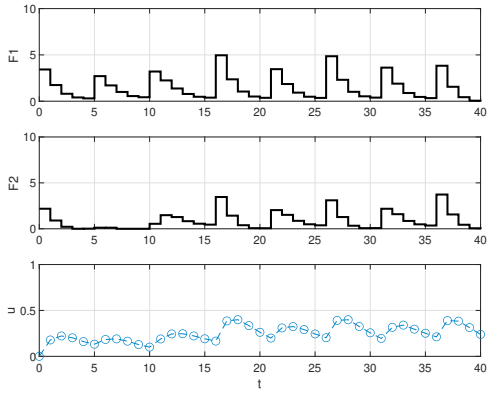

(b) Inputs and velocity u.

Fig. 2. The initial point of the trajectory is given by the ring in the center and the final point by the star. The controlled trajectory follows an spiral sequence of target sets given by squares.

Before presenting the exploration mission for water quality assessment some simulation scenarios will be presented to explore a region which is meshed by squares and by hexagons. To explore some of the main difference in the controlled trajectories two index will be used, the first index, I_F, computes the accumulative inputs for all the time of simulation, is define by the following:

$$I_F = \sum_{i=0}^{T_f} F_1(i) + F_2(i) \tag{10}$$

Index I_F resumes the consumption of energy for the thrust forces to complete the entire exploration.

The second index, I_S, penalize large changes on consecutive inputs. Is define as follows

$$I_S = \sum_{i=0}^{T_f-1} \|F_1(i+1) - F_1(i)\|^2 + \|F_2(i+1) - F_2(i)\|^2 \tag{11}$$

The idea of index I_S is to measure the smoothness of the inputs used to complete the exploration.

The parameters of the MPC is the same on all scenarios given by a prediction horizon $N = 15$, weight values on cost (7) given by $p = q = 1$ and $\alpha = 5, \beta = 0.1$.

Fig. 1 and Fig. 2 show a controlled trajectory for explore the same region that is meshed by hexagons and squares, respectively. The sequence of target sets Ω_j are ordered to follows a spiral trajectory, which in the case of hexagon meshing provide the best planning path (see Table 1). On the other hand, Fig. 3 and 4 show the same region and the same meshing but with a different path planing, in this case - according Table 1 - the square meshing is more appropriate.

INDEX	HEXAGON MESH	SQUARE MESH
I_F	73.6 (Fig. 1)	91.72 (Fig. 2)
I_S	100.38 (Fig. 1)	110.84 (Fig. 2)
I_F	133.37 (Fig.3)	165 (Fig. 4)
I_S	218.7 (Fig.3)	163 (Fig. 4)

Table 1: Index I_F and I_S for every path on Fig. 1-4.

6. WATER QUALITY ASSESSMENT BY USV TECHNOLOGY

The proposed MPC is used to control the SPYBOAT® vessel for explore a large area on the surface of Heron lake Villeneuve

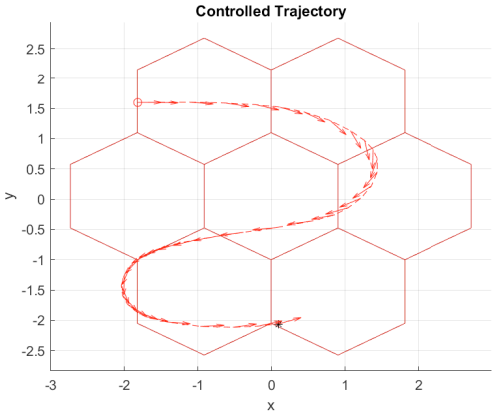

(a) Trajectory on hexagon meshing.

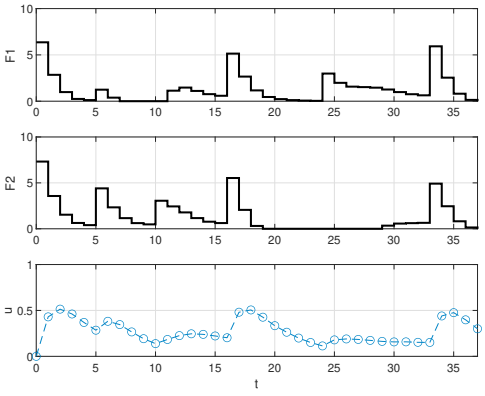

(b) Inputs and velocity.

Fig. 3. Hexagon meshing.

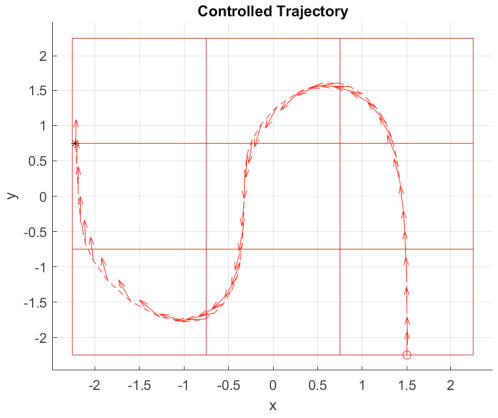

(a) Trajectory on square meshing.

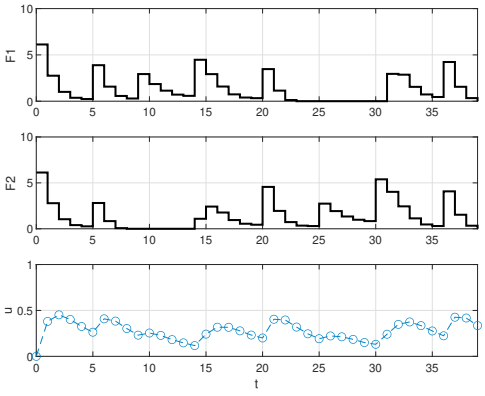

(b) Inputs and velocity.

Fig. 4. Square meshing.

d'Ascq (France). The real experiments were carried out by hand-operated USV to collect measurements of *pH, turbidity, conductivity, temperature and dissolved oxygen* in the entire area. The main problem of the hand-operated USV mission was the irregularity of the trajectory on the studied area, since the USV was controlled manually the route of the vessel leaves many places un-visited, and therefore and without data. To solve this problem, Anderson et al. (2022b) proposed a method for interpolation to approximate the missing data, but still shows some limitations.

To improve data collecting the proposed MPC is used to simulate the real experiment in the same region. Fig. 5 shows the application of the proposed nonlinear MPC with a prediction horizon $N = 10$, a discretization of the dynamical model (9) with discrete-time with $T = 1seg$ and initial state $x(0) = (x, y, \psi, u, v, r) = (146, 4, -\frac{pi}{2}, 0, 0, 0)$. To explore region Ω a regular mesh of hexagons. Every target set Ω_x shares an edge with the next target set Ω_x^+, so once the system enters Ω, only the second mode of the MPC (8) is used (the first mode is only used at the beginning to reach Ω_1). Fig. 6 shows a limnological map for Dissolved Oxygen. This map represent the measurement of the vessel in every target set $Omega_j$.

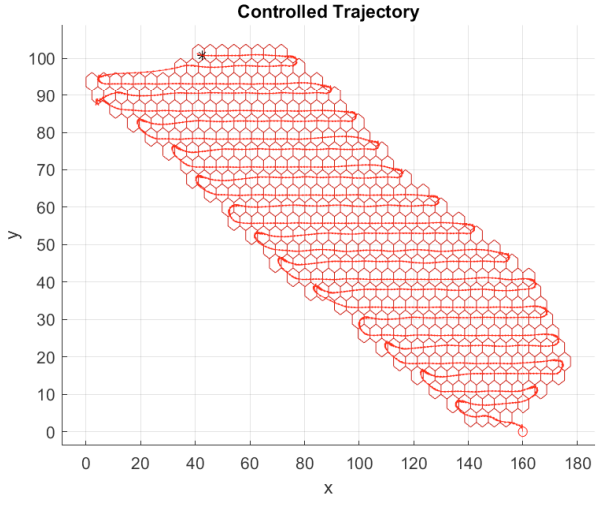

Fig. 5. Controlled trajectory for exploring region Ω.

7. CONCLUSION

A nonlinear MPC for exploration with USV was presented in this paper to improve the data collecting for the construction of a temporal water quality profile of a region of the surface of lakes where there is a suspicion of a source of pollution. This results are expected to outperformed the real exploration of large areas targeting data collection for water quality analysis.

ACKNOWLEDGMENT

Authors want to thanks the company Bathy drone Solutions (BDS) for its participation in the experiments, and the Department of Economic Transformation, Industry, Knowledge

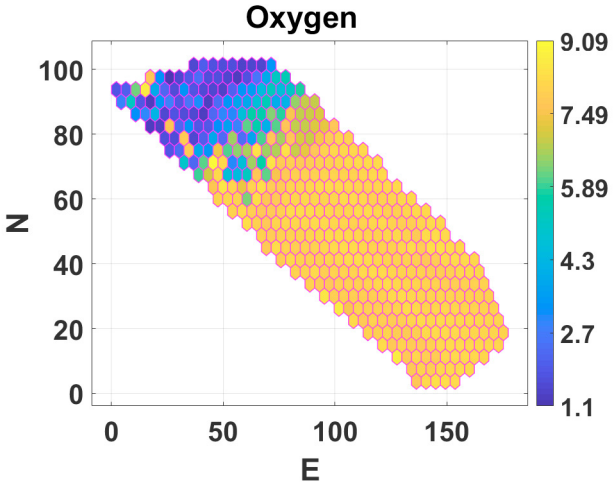

Fig. 6. Limnological map construction on Ω for the Dissolved Oxygen.

and Universities of the Andalusian Government (PAIDI 2020) [Ampliación Aquacollect, ref. P18-HO-4713].

REFERENCES

Anderson, A., Martin, J., Bouraqadi, N., Etienne, L., Langueh, K., Rajaoarisoa, L., Lozenguez, G., Fabresse, L., Maestre, J., and Duviella, E. (2022a). Nonlinear Set-based Model Predictive Control for Exploration: Application to Environmental Missions. URL https://hal.archives-ouvertes.fr/hal-03647736.

Anderson, A., Martin, J., Mougin, J., Bouraqadi, N., Duviella, E., Etienne, L., Fabresse, L., Langueh, K., Lozenguez, G., Alary, C., Billon, G., Superville, P., and Maestre, J. (2022b). Water Quality Map Extraction from Field Measurements Targetting Robotic Simulations. *IAMES-PapersOnLine*.

Blanchini, F. and Miani, S. (2015). *Set-Theoretic Methods in Control*. Systems & Control: Foundations & Applications. Springer International Publishing. URL https://books.google.com.ar/books?id=8a0YCgAAQBAJ.

Hervagault, Y. (2019). *Design and Implementation of an Effective Communication and Coordination System for Unmanned Surface Vehicles (USV)*. Ph.D. thesis, Université Grenoble Alpes.

Madeo, D., Pozzebon, A., Mocenni, C., and Bertoni, D. (2020). A low-cost unmanned surface vehicle for pervasive water quality monitoring. *IEEE Transactions on Instrumentation and Measurement*, 69(4), 1433–1444.

Martin, J., Maestre, J., and Camacho, E. (2021). Spatial Irradiance Estimation in a Thermosolar Power Plant by a Mobile Robot Sensor Network. *Solar Energy*, 220, 735–744.

Matschek, J., Bäthge, T., Faulwasser, T., and Findeisen, R. (2019). Nonlinear predictive control for trajectory tracking and path following: An introduction and perspective. In *Handbook of Model Predictive Control*, 169–198. Springer.

Mayne, D.Q., Rawlings, J.B., Rao, C.V., and Scokaert, P.O. (2000). Constrained model predictive control: Stability and optimality. *Automatica*, 36(6), 789–814.

Nascimento, T.P., Dórea, C.E., and Gonçalves, L.M.G. (2018). Nonholonomic mobile robots' trajectory tracking model predictive control: a survey. *Robotica*, 36(5), 676–696.

Sarunic, P. and Evans, R. (2014). Hierarchical model predictive control of uavs performing multitarget-multisensor tracking. *IEEE Transactions on Aerospace and Electronic Systems*, 50(3), 2253–2268.

Wang, Z., Yang, S., Xiang, X., Vasilijević, A., Mišković, N., and Na, . (2021). Cloud-based mission control of usv fleet: Architecture, implementation and experiments. *Control Engineering Practice*, 106, 104657.